Published in final edited form as:
Development. 2007 June ; 134(11): 2159–2169. doi:10.1242/dev.001586.

Conditional *Kif3a* ablation causes abnormal hedgehog signaling topography, growth plate dysfunction and ectopic cartilage formation in mouse cranial base synchondroses

Eiki Koyama[1], **Blanche Young**[1], **Yoshihiro Shibukawa**[1], **Motohiro Nagayama**[1], **Motomi Enomoto-Iwamoto**[1], **Masahiro Iwamoto**[1], **Yukiko Maeda**[2], **Beate Lanske**[2], **Buer Song**[3], **Rosa Serra**[3], and **Maurizio Pacifici**[1]

[1] Department of Orthopaedic Surgery, Thomas Jefferson University College of Medicine, Philadelphia, PA 19107

[2] Department of Developmental Biology, Harvard School of Dental Medicine, Boston, MA 02138

[3] Department of Cell Biology, University of Alabama at Birmingham, Birmingham, AL 35294

SUMMARY

The motor protein Kif3a and primary cilia regulate important developmental processes, but their roles in skeletogenesis remain ill defined. Here we created mice deficient in *Kif3a* in cartilage and focused on the cranial base and synchondroses. *Kif3a* deficiency caused cranial base growth retardation and dys-morphogenesis evident in neonatal animals by anatomical and μCT inspection. *Kif3a* deficiency also changed synchondrosis growth plate organization and function and the severity of these changes increased over time. By P7, mutant growth plates lacked typical zones of chondrocyte proliferation and hypertrophy and were instead composed of chondrocytes with an unusual phenotype characterized by strong *collagen II* expression, but barely detectable expression of *Indian hedgehog* (*Ihh*), *collagen X*, *VEGF*, *MMP-13* and *Osterix*. Concurrently, unexpected developmental events occurred in perichondrial tissues that included excessive intramembranous ossification and formation of ectopic cartilage masses. Looking for possible culprits for the latter, we analyzed hedgehog signaling by monitoring expression of hedgehog effectors *Patched-1* and *Gli-1* and hedgehog binding surface component *syndecan-3*. Compared to controls, signaling was quite feeble within mutant growth plates already by P0, but was actually higher and widespread all along mutant perichondrial tissues. Lastly, we studied postnatal mice deficient in *Ihh* in cartilage; their cranial base defects only minimally resembled those in *Kif3a*-deficient mice. In sum, Kif3a and primary cilia make unique contributions to cranial base and synchondrosis development and their deficiency causes growth plate dysfunction, abnormal topography of hedgehog signaling, and un-physiologic responses and processes in perichondrial tissues including ectopic cartilage formation and excess intramembranous ossification.

Keywords

Kif3a; primary cilia; cranial base synchondroses; growth plate; hedgehog signaling; intramembranous ossification; ectopic cartilage

INTRODUCTION

Kif3a is an essential component of the intraflagellar transport (IFT) motor system of primary cilia (Rosenbaum and Witman, 2002). These organelles are microtubule-containing non-motile structures protruding from the surface of most vertebrate cells that were first described decades ago (Scherft and Daems, 1967; Sorokin, 1968). Recent studies have shown that primary cilia

are important regulators of cell and tissue function and developmental processes. Mutations in primary cilia's structural and functional components can cause serious human conditions, including polycyctic kidney disease and retinal degeneration (Ansley et al., 2003; Lin et al., 2003; Pazour et al., 2000). Similarly, altered primary cilia function can have damaging repercussions on limb patterning, neural tube formation and other major developmental processes (Huangfu et al., 2003; Murcia et al., 2000; Zhang et al., 2003). The importance and centrality of primary cilia in both health and disease reflect the fact that these organelles and their IFT system have turned out to mediate and transduce intercellular chemical, physical and biological signals (Davenport and Yoder, 2005), including those elicited by hedgehog proteins (Corbit et al., 2005; Haycraft et al., 2005; May et al., 2005). These proteins are well known regulators of multiple developmental processes (Bitgood and McMahon, 1995; McMahon et al., 2003). They are lipid-containing factors secreted by donor cells that diffuse through the surroundings and exert action on short- and long-range target cells (Gritli-Linde et al., 2001; Yin et al., 2002). The proteins act by binding to the cell surface receptor Patched and signals are transmitted by the receptor Smoothened via zinc-finger transcription factors Gli1, Gli2 and Gli3. Current thinking reviewed recently (Huangfu and Anderson, 2006; Singla and Reiter, 2006) is that following hedgehog interaction with Patched, Smoothened is activated and translocated to primary cilia via the ITF system, resulting in production of Gli activator forms that would translocate to the nucleus and activate hedgehog gene target expression. In the absence of hedgehog proteins, Smoothened would remain sequestered and inactive, and Gli proteins would be processed into repressor forms and move to the nucleus to inhibit hedgehog target gene expression.

A well documented target of hedgehog signaling is the developing axial and limb skeleton (Bitgood and McMahon, 1995; Koyama et al., 1996; Lanske et al., 1996). As a recent study from our groups shows, hedgehog signaling is also very important for early formation, growth and function of the cranial base and its synchondroses (Young et al., 2006). The synchondroses are cartilaginous palindromic structures each consisting of two mirror-image growth plates and termed ethmoidal, intrasphenoidal, spheno-occipital and intraoccipital according to their anatomical location. They are important for cranial base development and overall growth patterns (Ingervall and Thilander, 1972; Roberts and Blackwood, 1983), and defects in synchondrosis functioning are likely to contribute to craniofacial deformities such as those seen in Crouzon and Apert syndromes (Chen et al., 1999; Kreiborg et al., 1993). We found that synchondrosis development is severely affected in mice lacking *Indian hedgehog*. The $Ihh^{-/-}$ cartilaginous cranial bases were short and deficient in extracellular proteoglycan matrix. The mutant synchondroses displayed abnormal chondrocyte proliferation, hypertrophy and topographical arrangement with respect to perichondrium; as a consequence, endochondral ossification was deranged. In several but not all respects, these abnormalities are reminiscent of those seen in developing $Ihh^{-/-}$ long bones (St-Jacques et al., 1999), pointing to the pivotal nature and general requirement of hedgehog action in skeletogenesis. Given their roles in hedgehog signaling, primary cilia should be as essential for skeletal development and growth, and previous genetic studies certainly support that premise (Murcia et al., 2000; Zhang et al., 2003). Recent reports have described skeletal abnormalities in limbs, calvaria and cranial base in conditional mouse mutants lacking *Kif3a* or cilia-associated mechanosensor protein *polycyctin-1* genes and mice with a missense mutation in the *Pc1* gene (Olsen et al., 2005; Xiao et al., 2006), but the specific roles and functions of primary cilia in skeletogenesis and cartilage and growth plate function are still unclear. To obtain such insights and information, we created mice deficient in Kif3a in cartilage and focused on the cranial base and synchondroses, aiming to establish also whether and to what extent defects due to ciliary malfunction compare with those due to hedgehog malfunction. We find that the *Kif3a*-deficient cranial bases are abnormal and display both predicted and unexpected defects, the latter including a severe failure of hypertrophic cartilage formation, disregulation of hedgehog

signaling topography and emergence of ectopic cartilage masses and excess intramembranous bone.

MATERIALS AND METHODS

Conditional *Kif3a* and *Ihh* ablation

Animals used in this study were maintained in accordance with the NIH Guide for the Care and Use of Laboratory Animals, and protocols were reviewed and approved by the IACUC at each of our respective Institutions. Homozygous mice deficient in *Kif3a* in cartilage were produced by sequential mating of $Kif3a^{fl/fl}$ mice (Marszalek et al., 1999) with *Col2a1-Cre* transgenic mice (Ovdhinnikov et al., 2000). The genotype of transgenic mice was determined by PCR analyses of genomic DNA isolated from tail or liver. The *Col2a1-Cre* mice were identified by using Primer1: 5′ TGC TCT GTC CGT TTG CCG 3′ and Primer2: 5′ ACT GTG TCC AGA CCA GGC 3′, generating one band of about 720 bp. The *loxP* alleles or *Kif3a* were identified using three primers: Primer1: 5′ TCT GTG AGT TTG TGA CCA GCC 3′; Primer2: 5′ AGG GCA GAC GGA AGG GTG G 3′; and Primer 3: 5′ TGG CAG GTC AAT GGA CGC AG 3′. Homozygous Kif3a-deficient mice were born with Mendelian frequency and were studied at postnatal stages P0, P7 and P15.

Homozygous mice deficient in *Ihh* in postnatal cartilage were produced by sequential mating $Ihh^{fl/fl}$ mice (Maeda et al., 2006) with *Col2a1-CreER* transgenic mice (Nakamura et al., 2006). Genotyping of mice was performed by PCR using the following specific primers: *fl-Ihh* forward 5′-AGC ACC TTT TTT CTC GAC TGC CTG- 3′, *fl-Ihh* reverse 5′-TGT TAG GCC GAG AGG GAT TTC GTG-3′; *Cre 275 5′*-CGC GGT CTG GCA GTA AAA ACT ATC-3′, *Cre 603 5′*-CCC ACC GTC AGT ACG TGA GAT ATC- 3′. After an initial denaturation for 8 min at 94°C, amplification cycles consisted of denaturation at 94°C for 30 sec, annealing at 68°C for 30 sec, and 45 sec extension at 72°C for 35 cycles, followed by a final extension for 10 min at 72°C. The expected amplicons for the wild type *Ihh* allele were 320 bp, for the floxed *Ihh* allele 400 bp, and for the *Cre* allele 328 bp. To verify Cre activity and specificity postnatally, *Col2a1-CreER* mice were mated with Rosa R26R reporter mice, and resulting double transgenic mice were injected with 4-hydroxy-tamoxifen (Sigma) at P0 and evaluated for *LacZ* activity at P1, P4, P7 and P14 by histochemistry (Nakamura et al., 2006).

Micro computed tomography, histology and immunohistochemistry

Skulls were fixed in buffered 4% paraformaldehyde overnight at 4°C, rinsed and subjected to micro computed tomography (μCT) using a μCT40 SCANCO Medical system. Samples were scanned using a 36 mm holder at 45 kvolts of energy, 12 μm scanning thickness and medium resolution. Two dimensional slice images were selected and used to generate three dimensional reconstructions with the following parameters: filter width sigma = 0.8, support level = 1.0, and threshold =173. The same values were used to analyze wild type and mutant samples at each specified time point. Three-dimensional images were rotated at specific angles to generate lateral and bird-eye views of the cranial base.

For histology and immunohistochemistry, fixed skulls were rinsed in DEPC-treated water and decalcified in 0.1M Tris, pH 7.5 buffer containing 0.1% DEPC, 10% EDTA-4 Na, and 7.5% polyvinyl pyrolidione (PVP). For routine histological analysis, 5 mm sections were stained with hematoxylin and eosin or fast green using standard procedures. For immunofluorescence staining, 10 μm sections were incubated with 1:200 dilution of anti-acetylated α-tubulin monoclonal antibody (Sigma, Clone 6-11B-1) followed by biotinylated secondary antibodies and Cy3 conjugated streptavidin (Vector laboratories) to yield signal. Sections were

counterstained with YOPRO••-3 iodide (612/631) or 4′,6-diamidino-2-phenylindole dihydrochloride (DAPI) (Invitrogen) to reveal nuclei.

Gene expression analysis

Serial paraffin tissue sections were pretreated with 10 μg/ml proteinase K (Sigma) for 10 min at room temperature, post-fixed in 4% paraformaldehyde, washed with PBS containing 2 mg/ml glycine, and treated with 0.25% acetic anhydride in triethanolamine buffer (Koyama et al., 1996). Sections were hybridized with antisense or sense ^{35}S-labeled probes (approximately 1×10^6 DPM/section) at 50°C for 16 hrs. Mouse cDNA clones included: histone H4C (nt. 549–799; AY158963); PTHrP (nt. 66–1386; NM_008970); osteopontin (nt. 1–267; AF515708); *Osterix* (nt. 40–1727; NM_130458); VEGF (nt. 115–539; gi/249858); *Ihh* (nt. 897–1954; MN_010544); *Patched-1* (nt. 81–841; NM_008957); *Smoothened* (nt. 450–1000; BC048091); collagen X (nt. 1302–1816; NM009925); and collagen II (nt. 1095–1344; X57982). After hybridization, slides were washed with 2X SSC containing 50% formamide at 50°C, treated with 20 μg/ml RNase A for 30 min at 37°C, and washed three times with 0.1X SSC at 50°C for 10 min/wash. Sections were dehydrated with 70, 90, and 100% ethanol for 5 min/step, coated with Kodak NTB-3 emulsion diluted 1:1 with water, and exposed for 10 to 14 days. Slides were developed with Kodak D-19 at 20°C and stained with hematoxylin. Dark and bright field images were captured using a digital camera, and dark field images were pseudo-colored using Adobe Photoshop software.

RESULTS

Cranial base and synchondroses are abnormal in conditional *Kif3a*-deficient mice

Gross anatomical inspection showed that the craniofacial skeleton was indeed defective in *Kif3a*$^{fl/fl}$*;Col2a1-Cre* mice (heretofore termed *Kif3a*-deficient mice) compared to *Kif3a*$^{fl/wt}$*;Col2a1-Cre* and *Kif3a*$^{fl/fl}$ mice (heretofore termed control mice) particularly at postnatal stages. Thus, we processed the skulls of P0, P7 and P15 mice for μCT and histology, focusing on the cranial base. Control cranial bases displayed a typical elongated morphology along the antero-posterior axis (Fig. 1A) and their intrasphenoidal (*is*), spheno-occipital (*so*) and intra-occipital (*io*) synchondroses were well defined and distinct (Fig. 1B). Histologically, the synchondroses were fully cartilaginous reflecting their active growth status and flanked intervening regions of endochondral bone (Fig. 1C,D,E). In contrast, P7 *Kif3a*-deficient cranial bases were wider than controls (Fig. 1H), and their synchondroses were deformed (Fig. 1I) and even exhibited segments of mineralized tissue bridging the neighboring bones (Fig. 1I, arrows), a potentially catastrophic defect that would hamper growth. Their overall histological organization and shape were already defective at P0 (Fig. 1J) and much more so at P7 and P15 (Fig. 1K,L), and length of the intervening bone region was markedly decreased (Fig. 1E,L, horizontal bars) reflecting cranial base's shortening along its antero-posterior axis. Immunostaining with antibodies to acetylated α-tubulin confirmed that primary cilia were obvious in control chondrocytes (Fig. 1F, arrowheads) but rare in *Kif3a*-deficient chondrocytes (Fig. 1M, arrowhead), attesting to effectiveness of *Col2a1-Cre* action. In addition, primary cilia were equally evident in perichondrial tissue of both control and *Kif3a*-deficient cranial bases (Fig. 1G,N, arrowheads), attesting to specificity of *Col2a1-Cre* action clearly limited to cartilage.

Gene expression analysis reveals dysfunction of mutant growth plates

Upon closer microscopic inspection, control synchondroses such as the spheno-occipital synchondrosis (Fig. 2A) displayed characteristic growth plate zones of small round resting chondrocytes (Fig. 2B, *rz*), flat shaped proliferating chondrocytes (Fig. 2B, *pz*), and oval pre-hypertrophic chondrocytes and large mature hypertrophic chondrocytes (Fig. 2C, *phz* and *hz*) followed by primary bone spongiosa intermixing with marrow (Fig. 2D, arrowheads). In sharp

contrast, *Kif3a*-deficient growth plates lacked well-defined zones (Fig. 2I). In particular, small-sized resting and flat-shaped chondrocytes were conspicuously absent; instead, a mixed population of slightly enlarged and oval-to-round chondrocytes was present (Fig. 2J,K). In addition, the hypertrophic zone was very small (Fig. 2K), and there was an abrupt transition from cartilage to marrow and a concurrent reduction in primary spongiosa and endochondral bone (Fig. 2L) (Xiao et al., 2006). In line with absence of flat-shaped cells, mutant growth plates contained few proliferating chondrocytes as indicated by gene expression of mitotic marker histone 4C, (Fig. 2M,N,O), while the cells were abundant and organized in two distinct proliferative zones in control growth plates (Fig. 2E,F,G, arrowheads). Indeed, gene expression of *PTHrP*, a major regulator of growth plate chondrocyte proliferation (Lanske et al., 1996;Vortkamp et al., 1996), was strong in controls (Fig. 2H), but was low in mutant growth plates (Fig. 2P).

Growth plate disorganization and deficiency in primary spongiosa and endochondral bone suggested that the chondrocyte maturation process had been deranged in *Kif3a*-deficient synchondroses. In situ hybridization showed that compared to controls, the mutant chondrocytes did express low levels of *Ihh* and *collagen X* that are characteristic products of pre-hypertrophic and early hypertrophic chondrocytes (Fig. 3B,C,G,H), and equally low levels of *MMP-13* and *VEGF* that are important for cartilage-to-endochondral bone transition (Fig. 3D,E,I,J) (Engsig et al., 2000; Zelzer et al., 2002). Deficiency in primary spongiosa (Fig. 4F) was reflected in the fact that expression of such bone markers and regulators as *osteopontin*, *collagen I*, *Runx2* and *Osterix* was quite low in mutant (Fig. 4G,H,I,J) versus control specimens (Fig. 4B,C,D,E). Despite all these serious changes, mutant chondrocytes still exhibited strong *collagen II* expression as controls did (Fig. 3A,F), signifying that their basic differentiated phenotype was largely preserved.

Excessive intramembranous ossification and ectopic cartilage formation

As they develop and mature in the growth plate, pre-hypertrophic and hypertrophic chondrocytes induce formation of intramembranous bone in adjacent perichondrial tissues, a process due to *Ihh* (Koyama et al., 1996; Nakamura et al., 1997; St-Jacques et al., 1999). Control synchondroses such as the spheno-occipital synchondrosis, conformed to this general rule. It displayed fast green-positive intramembranous bone flanking the *Ihh*-rich pre- and hypertrophic zones (Fig. 5A, arrowhead) and expressing *collagen I*, *Runx2* and *Osterix* (Fig. 5B,C,D, arrowheads); importantly, there was no appreciable bone flanking the proliferative and resting zones as to be expected (Fig. 5A,B,C,D, arrows). In contrast, intramembranous bone had formed all along the growth plate in companion *Kif3a*-deficient synchondrosis, thus spanning the entire flank of the synchondrosis and bridging the neighboring occipital and sphenoidal bones (Fig. 5E,F,G,H). This excess intramembranous bone undoubtedly corresponds to the regions of mineralized tissue initially detected by μCT (Fig. 1I, arrows) and appreciable also by general histology (Fig. 1K,L, double arrowheads).

Based on these findings, we asked whether there might be additional aberrations occurring in perichondrial tissues flanking *Kif3a*-deficient synchondroses. Further scrutiny did reveal that, surprisingly, ectopic cartilage masses had formed at several sites (Fig. 6D,E,F, arrows). The tissue was recognizable by its characteristic histology as well as *collagen II* gene expression and was located almost invariably in close proximity to the mutant synchondrosis growth plates (Fig. 6D,E,F, arrows), thus displaying a topographical arrangement also seen in pathological exostoses that form in close proximity of growth plates (Hecht et al., 1995). Ectopic cartilage masses were never seen in tissues flanking control synchondroses and their chondro-perichondrial boundary was extremely well defined and un-violated (Fig. 6A,B,C).

Aberrant topography of hedgehog signaling

What could have triggered excessive intramembranous ossification and ectopic cartilage formation near mutant growth plates? An obvious possibility was that hedgehog signaling, and in particular the topography of signaling, had changed in mutant specimens, triggering broader responses in neighboring perichondrial tissues. To test this possibility, we determined the expression patterns of *Ihh* and its target genes *Patched-1* and *Gli1* in control and *Kif3a*-deficient synchondroses. We chose to focus on P0 hoping to detect as early changes in signaling patterns as possible. In controls, the three genes displayed predictable and distinct expression patterns, with abundant *Ihh* transcripts in pre-hypertrophic zones (*phz*) (Fig. 7A,B,G,H) and *Patched-1* and *Gli1* transcripts in preceding proliferative zones (*pz*) (Fig. 7C,D,I,J), reflecting the well established role of Ihh in chondrocyte proliferation (Shimo et al., 2004; St-Jacques et al., 1999). There was also clear *Patched-1* and *Gli1* expression in perichondrial tissue flanking the pre-hypertrophic and hypertrophic zones where the intramembranous bone collar normally forms (Fig. 7C,D,I,J, single arrowhead), but perichondrium flanking the resting and proliferative zones was negative (Fig. 7C,D,I,J, double arrowhead). *Smoothened* transcripts were present throughout the growth plates (Fig. 7E,K). In mutant synchondroses, *Ihh* expression was still strong at this stage (Fig. 7M,N,S,T), but expression of both *Patched-1* and *Gli1* was grossly abnormal. *Patched-1* and *Gli-1* transcripts were very low and scattered within the growth plates (Fig. 7O,P,U,V) but were evident along the entire length of perichondrial tissues (Fig. 7O,P,U,V, arrowhead), thus closely mirroring the location of excessive intramembranous bone formation. *Smoothened* expression appeared largely unaffected (Fig. 7Q,W).

To reinforce the idea that hedgehog signaling topography may be altered in mutant synchondroses, we asked whether expression of molecules needed to direct and restrict hedgehog signaling was altered as well. We focused on heparan sulfate proteoglycans known for their pivotal roles in hedgehog signaling logistics (Bellaiche et al., 1998; The et al., 1999) and on syndecan-3 in particular that we found to participate in such roles in long bone growth plates (Shimazu et al., 1996; Shimo et al., 2004). In controls, *Syndecan-3* was expressed in the proliferative zones of synchondrosis growth plates (Fig. 7F,L) along with *Patched-1* and *Gli-1*, in line with the idea that this syndecan may direct and limit Ihh action on proliferation (Pacifici et al., 2005). However, there was barely detectable *syndecan-3* expression in *Kif3a*-deficient synchondroses (Fig. 7R,X).

Skeletal aberrations are caused by postnatal *Ihh* deficiency

The severe cranial base and synchondrosis abnormalities triggered by *Kif3a* deficiency in cartilage raised the question of whether they had a unique character or would resemble those elicited by deficiency in related genes, such as *Ihh*. Accordingly, we created conditional postnatal mice lacking *Ihh* in cartilage by treating neonatal $Ihh^{fl/fl}$*;Col2a-CreER* mice with tamoxifen. Mice were sacrificed at P7 and P15 (heretofore termed *Ihh*-deficient mice); neonatal $Ihh^{fl/fl}$ littermates were treated with tamoxifen in parallel and served as controls. *Ihh*-deficient skulls exhibited antero-posterior shortening and abnormal synchondroses (Fig. 8E) relative to controls (Fig. 8E) reminiscent of the defects seen in *Kif3a*-deficient skulls above. At variance with the latter, however, the *Ihh*-deficient growth plates were entirely occupied by collagen X-expressing hypertrophic chondrocytes (Fig. 8F) and there was no detectable intramembranous ossification in flanking perichondrial tissues (Fig. 8G, arrowhead) relative to control (Fig. 8B,C). Defects were exacerbated by P15 when much of *Ihh*-deficient synchondroses had been replaced by endochondral bone and marrow and remnants of growth plate tissue were confined to a lateral and inconspicuous position (Fig. 8H), phenomena not seen in P15 *Kif3a*-deficient specimens.

DISCUSSION

In this study, we provide evidence that Kif3a and primary cilia are pivotal for cranial base and synchondrosis development and function. *Kif3a* deficiency alters the antero-posterior and lateral growth patterns of the cranial base, resulting in skull dys-morphogenesis reminiscent of defects seen in some Apert and Crouzon patients (Kreiborg et al., 1993). *Kif3a* deficiency affects as severely the behavior and functional organization of synchondrosis growth plates, resulting in a quasi-stasis of the chondrocyte maturation process and retardation of endochondral bone formation. Concurrently, there were unexpected and unpredicted alterations in developmental events occurring in synchondrosis perichondrial tissues that include excessive intramembranous ossification, most likely impacting very negatively on cranial base growth. Only some of these defects resemble those caused by conditional deficiency of *Ihh*, indicating that Kif3a and primary cilia make unique contributions to normal progression of cranial base and synchondrosis development, organization and function.

Growth plates are complex multi-facet structures in which chondrocyte shape, orientation and polarity, chondrocyte proliferation and phenotype, and chondrocyte maturation and hypertrophy must all be regulated in a coordinated manner. A well established mechanism delineated by work on developing long bones is the PTHrP-Ihh axis in which PTHrP produced by periarticular cells under Ihh influences regulates the rates of chondrocyte proliferation (Lanske et al., 1996). In line with this model, *Ihh* gene ablation in mouse embryos causes down-regulation of *PTHrP* expression and reduced proliferation (St-Jacques et al., 1999). This mechanism can certainly account for the decrease in chondrocyte proliferation in *Kif3a*-deficient growth plates that express low if any PTHrP. This would imply that synchondroses conform to, and obey, the PTHrP-Ihh axis (Young et al., 2006) and that a normal complement of Kif3a and primary cilia is needed to maintain it. Reduced proliferation was accompanied by absence of flat-shaped chondrocytes normally constituting the proliferative zone, absence of distinct resting, pre-hypertrophic and hypertrophic zones, and absence of a columnar cell organization. Such nearly chaotic organization of *Kif3a*-deficient growth plates thus suggests that the mutant chondrocytes may lack key topographical, navigational or mechanical mechanisms and devices that enable them to perceive location or cues within the growth plate and adopt appropriate zone-specific polarity, shape and phenotype. One such mechanism could be the planar cell polarity pathway (PCP), a form of non-canonical Wnt pathway mediated by primary cilia that is essential for cell orientation and mitotic spindle alignment in organs such as inner ear, kidney tubules and cranial cartilage (Dabdoub and Kelley, 2005; Fisher et al., 2006; Park et al., 2006). Importance and centrality of the PCP pathway in several systems make it likely that it operates in growth plates as well (Olsen et al., 2005) where it could orient chondrocyte mitotic spindle and division plane that are usually perpendicular to growth plate's longitudinal axis (Dodds, 1930) or could promote the related process of columnar organization. Notably, since both PCP pathway and hedgehog proteins act via primary cilia, chondrocytes could control their polarity and orientation in relation to, and correlation with, their responses to Ihh which is distributed in the form of gradients within the growth plate (Gritli-Linde et al., 2001; Yin et al., 2002).

In addition to being disorganized, the *Kif3a*-deficient growth plates are occupied by enlarged oval-round chondrocytes that express *collagen II* but little if any maturation genes including *collagen X*, and are followed by a poor primary bone spongiosa. These phenotypic defects are rather unusual and clearly different from those seen in prenatal *Ihh*-null synchondroses (Young et al., 2006) or postnatal *Ihh*-deficient synchondroses described here in which there is exuberant and widespread chondrocyte hypertrophy followed by endochondral bone. One possibility is that the *Kif3a*-deficient chondrocytes are unable to respond to factors that promote their maturation and hypertrophy, including β-catenin-dependent Wnt proteins (Enomoto-Iwamoto et al., 2002; Tamamura et al., 2005) whose signaling and action may involve primary cilia

(Germino, 2005). Alternatively, the topographical disorganization discussed above could have led to general intermingling and intermixing of chondrocytes with different phenotypic properties and maturation status within the mutant growth plates, creating conditions in which the cells interfere with each other's phenotype. Previously, we showed that when immature chondrocytes are co-cultured with hypertrophic chondrocytes, the hypertrophic phenotype is suppressed (D' Angelo and Pacifici, 1997).

One of the most intriguing and unexpected defects seen in *Kif3a*-deficient synchondroses is formation of excessive intramembranous bone and ectopic cartilage masses both readily appreciable by P7. These defects are preceded by alteration in hedgehog signaling topography delineated by *Patched-1* and *Gli-1* expression along the entire length of perichondrial tissues. Given that hedgehog proteins can stimulate osteogenesis and chondrogenesis (Enomoto-Iwamoto et al., 2000; Nakamura et al., 1997), excess hedgehog signaling in perichondrial tissues could have directly caused excessive intramembranous bone and cartilage formation. What remains unclear, however, is why there is excess signaling all along perichondrium to begin with, particularly starting at P0 when *Ihh* expression is still confined to fairly-restricted growth plate zones (see Fig. 7). One possibility is that the excess signaling is an autonomous local response of perichondrium to phenotypic defects in the adjacent growth plates. Alternatively, it could be due to the mutant chondrocytes themselves. For example, the *Kif3a*-deficient chondrocytes may lack means to control location and distribution of Ihh, allowing it to diffuse broadly and reach the entire length of perichondrium. This hypothesis is indirectly sustained by our observation that the *Kif3a*-deficient growth plates express little if any syndecan-3, likely to be a component of mechanisms limiting and restricting Ihh diffusion and action in the growth plate (Pacifici et al., 2005; Shimo et al., 2004).

At this regard, it is interesting to point out a recent study with mice lacking one allele of *Ext2*, a Golgi-associated glycosyltransferase needed for heparan sulfate synthesis (Stickens et al., 2005). The *Ext2* heterozygous mice were found to be deficient in heparan sulfate and exhibited ectopic cartilaginous masses near their growth plates, thus mimicking exostoses present in Hereditary Multiple Exostosis patients who often have *EXT-2* or *EXT-1* mutations and reduced heparan sulfate levels (Hecht et al., 1995). The exact link between heparan sulfate deficiency and exostosis formation is still poorly understood. In the *Ext2* study above, it was proposed that heparan sulfate deficiency reduces FGF signaling and tilts the balance in favor of BMP signaling, resulting in chondrocyte misbehavior, weakening of the bone collar, and formation of exostosis masses (Stickens et al., 2005). Our data showing reduced syndecan-3 expression in growth plate and excess hedgehog signaling in flanking perichondrial tissues point to hedgehog proteins and defective Kif3a-related mechanisms as culprits in exostosis formation as well. We do not know, however, how *Kif3a* deficiency and lack of primary cilia lead to a reduction in syndecan-3 expression. In previous studies, we did find that syndecan-3 over-expression in vivo and in vitro causes excess and widespread *Ihh* expression, suggesting that the two genes are coordinated and that such coordination was disrupted by *Kif3a* deficiency (Pacifici et al., 2005; Shimo et al., 2004). It will interesting to clarify whether *Kif3a* deficiency also affects expression of *syndecan-4* and *syndecan-2* that are normally expressed in proliferative zone and perichondrial tissues, respectively (David et al., 1993; Pacifici et al., 2005) and/or expression of other heparan sulfate proteoglycans including glypicans and perlecan. Given that hedgehogs, BMPs, FGFs and Wnts are all heparan sulfate-binding factors (Bernfield et al., 1999), the data may provide insights into how the various proteoglycans with their distinct structures and expression patterns may help to mediate and coordinate the functions of the many signaling factors and pathways that converge to orchestrate progression of skeletal development and how defects in these circuits could cause pathologies including HME.

Acknowledgments

This work was supported by NIH grants AR047543, AR046000 and AR050560

References

Ansley SJ, Badano JL, Blacque OE, Hill J, Hoskins BE, Leitch CC, Kim JC, Ross AJ, Eichers ER, Teslovich TM, et al. Basal body dysfunction is a likely cause of pleiotropic Bardet-Biedl syndrome. Nature 2003;425:628–633. [PubMed: 14520415]

Bellaiche Y, The I, Perrimon N. Tout-velu is a Drosophila homologue of the putative tumor suppressor EXT-1 and is needed for Hh diffusion. Nature 1998;394:85–88. [PubMed: 9665133]

Bernfield M, Gotte M, Park PW, Reizes O, Fitzgerald ML, Lincecum J, Zako M. Functions of cell surface heparan sulfate proteoglycans. Annu Rev Biochem 1999;68:729–777. [PubMed: 10872465]

Bitgood MJ, McMahon AP. Hedgehog and Bmp genes are coexpressed at many diverse sites of cell-cell interaction in the mouse embryo. Dev Biol 1995;172:126–138. [PubMed: 7589793]

Chen L, Adar R, Yang X, Monsonego EO, Cuiling L, Hauschka PV, Yayon A, Deng CX. Gly369Cys mutation in mouse FGFR3 causes achrondroplasia by affecting both chondrogenesis and osteogenesis. J Clin Invest 1999;104:1517–1525. [PubMed: 10587515]

Corbit KC, Aanstad P, Singla V, Norman AR, Stainier DYR, Reiter JF. Vertebrate Smoothened functions at the primary cilium. Nature 2005;437:1018–1021. [PubMed: 16136078]

D' Angelo M, Pacifici M. Articular chondrocytes produce factors that inhibit maturation of sternal chondrocytes in serum-free agarose cultures: a TGFβ independent process. J Bone Min Res 1997;12:1368–1377.

Dabdoub A, Kelley MW. Planar cell polarity and a potential role for a Wnt morphogen gradient in stereociliary bundle orientation in the mammalian inner ear. J Neurobiol 2005;64:446–457. [PubMed: 16041762]

Davenport JR, Yoder BK. An incredible decade for the primary cilium: a look at a once-forgotten organelle. Am J Physiol Renal Physiol 2005;289:F1159–F1169. [PubMed: 16275743]

David G, Bai XM, vad der Schueren B, Marynen P, Cassiman JJ, van der Berghe H. Saptial and temporal changes in the expression of fibroglycan (syndecan-2) during mouse embryonic development. Development 1993;119:841–854. [PubMed: 8187643]

Dodds GS. Row formation and other types of arrangment of cartilage cells in endochondral ossification. Anat Rec 1930;46:385–399.

Engsig MT, Chen QJ, Vu TH, Pedersen AC, Therkidsen B, Lund LR, Henriksen K, Lenhard T, Foged NT, Werb Z, et al. Matrix metalloproteinase 9 and vascular endothelial growth factor are essential for osteoclast recruitment into developing long bones. J Cell Biol 2000;151:879–889. [PubMed: 11076971]

Enomoto-Iwamoto M, Kitagaki J, Koyama E, Tamamura Y, Wu C, Kanatani N, Koike T, Okada H, Komori T, Yoneda T, et al. The Wnt antagonist Frzb-1 regulates chondrocyte maturation and long bone development during limb skeletogenesis. Dev Biol 2002;251:142–156. [PubMed: 12413904]

Enomoto-Iwamoto M, Nakamura T, Aikawa T, Higuchi Y, Yuasa T, Yamaguchi A, Nohno T, Noji S, Matsuya T, Kurisu K, et al. Hedgehog proteins stimulate chondrogenic cell differentiation and cartilage formation. J Bone Min Res 2000;15:1659–1668.

Fisher, EEl; Doyen, A.; Nato, F.; Nicolas, JF.; Torres, V.; Yaniv, M.; Pontoglio, M. Defective planar cell polarity in polycystic kidney disease. Nature Genet 2006;38:21–23. [PubMed: 16341222]

Germino GG. Linking cilia to Wnts. Nature Genet 2005;37:455–457. [PubMed: 15858588]

Gritli-Linde A, Lewis P, McMahon AP, Linde A. The whereabouts of a morphogen: direct evidence for short- and graded long-range activity of hedgehog signaling peptides. Dev Biol 2001;236:364–386. [PubMed: 11476578]

Haycraft CJ, Banizs B, Aydin-Son Y, Zhang Q, Michaud EJ, Yoder BK. Gli2 and Gli3 localize to cilia and require intraflagellar transport protein Polaris for processing and function. PLoS Genetics 2005;1:480–488.

Hecht JT, Hogue D, Strong LC, Hansen MF, Blanton SH, Wagner H. Hereditary multiple exostosis and chondrosarcoma: linkage to chromosome II and loss of heterozygosiity for EXT-linked markers on chromosome II and 8. Am J Hum Genet 1995;56:1125–1131. [PubMed: 7726168]

Huangfu D, Anderson KV. Signaling from Smo to Ci/Gli: conservation and divergence of hedgehog pathways from Drosophila to vertebrates. Development 2006;133:3–14. [PubMed: 16339192]

Huangfu D, Liu A, Rakeman AS, Murcia NS, Niswander L, Anderson KV. Hedgehog signaling in the mouse requires intraflagellar transport proteins. Nature 2003;426:83–87. [PubMed: 14603322]

Ingervall B, Thilander B. The human spheno-occipital synchondrosis. I. The time of closure appraised macroscopically. Acta odontol Scand 1972:30.

Koyama E, Leatherman JL, Noji S, Pacifici M. Early chick limb cartilaginous elements possess polarizing activity and express *Hedgehog*-related morphogenetic factors. Dev Dynam 1996;207:344–354.

Kreiborg S, Marsh JL, Cohen MM, Liversage M, Pedersen H, Skovby F, Borgesen SE, Vannier MW. Comparative three-dimensional analysis of CT-scans of the calvaria and cranila base in Apert and Crouzon syndromes. J Craniomaxillofac Surg 1993;21:181–188. [PubMed: 8360349]

Lanske B, Karaplis AC, Lee K, Lutz A, Vortkamp A, Pirro A, Karperien M, Defize LHK, Ho C, Mulligan R, et al. PTH/PTHrp receptor in early development and Indian hedgehog-regulated bone growth. Science 1996;273:663–666. [PubMed: 8662561]

Lin FTH, Cordes K, Siclair AM, Goldstein LS, Somlo S, Igarashi P. Kidney-specific inactivation of the KIF3A subunit of kinesin-II inhibits renal ciliogenesis and produces polycystic kidney disease. Proc Natl Acad Sci USA 2003;100:5286–5291. [PubMed: 12672950]

Maeda Y, Suva LJ, Lanske B. Indian hedgehog (Ihh) is required for endochondral bone formation after birth. J Bone Min Res 2006;21:S40.

Marszalek JR, Ruiz-Lozano P, Roberts E, Chen KR, Goldstein LS. Situs inversus and embryonic ciliary morphogenesis defects in mouse mutants lacking the KIF3A subunit of kinesin-II. Proc Natl Acad Sci USA 1999;96:5043–5048. [PubMed: 10220415]

May SR, Ashique AM, Karlen M, Wang B, Shen Y, Zarbalis K, Reiter JF, Ericson J, Peterson AS. Loss of retrograde motor for IFT disrupts localization of Smo to cilia and prevents the expression of both activator and repressor functions of Gli. Dev Biol 2005;287:378–389. [PubMed: 16229832]

McMahon AP, Ingham PW, Tabin CJ. Developmental roles and clinical significance of hedgehog signaling. Curr Top Dev Biol 2003;53:1–114. [PubMed: 12509125]

Murcia NS, Richards WG, Yoder BK, Mucenski ML, Dunlap JR, Woychik RP. The Oak Ridge Polycyctic Kidney (orpk) disease gene is required for left-right axis determination. Development 2000;127:2347–2355. [PubMed: 10804177]

Nakamura E, Nguyen MT, Mackem S. Kinetics of tamoxifen-regulated Cre activity in mice using a cartilage-specific CreER^{T} to assay temporal activity windows along the proximodistal limb skeleton. Dev Dyn 2006;235:2603–2612. [PubMed: 16894608]

Nakamura T, Aikawa T, Enomoto-Iwamoto M, Iwamoto M, Higuchi Y, Pacifici M, Kinto N, Yamaguchi A, Noji S, Kurisu K, et al. Induction of osteogenic differentiation by hedgehog proteins. Biochem Biophys Res Commun 1997;237:465–469. [PubMed: 9268735]

Olsen BR, Kolpakova E, McBratney-Owen B, Li X, Zhou J, Fukai N. Genetic and epigenetic determinants of skeletal morphogenesis - Role of cellular polarity and ciliary function in skeletal development and growth. Oral Biosci Med 2005;213:57–65.

Ovdhinnikov DA, Deng JM, Ogunrinu G, Behringer RR. Col2a1-directed expression of Cre recombinase in differentiating chondrocytes in transgenic mice. Genesis 2000;26:145–146. [PubMed: 10686612]

Pacifici M, Shimo T, Gentili C, Kirsch T, Freeman TA, Enomoto-Iwamoto M, Iwamoto M, Koyama E. Syndecan-3: a cell surface heparan sulfate proteoglycan important for chondrocyte proliferation and function during limb skeletogenesis. J Bone Min Metab 2005;23:191–199.

Park TJ, Haigo SL, Wallingford JB. Ciliogenesis defects in embryos lacking inturned or fuzzy function are associated with failure of planar cell polarity and hedgehog signaling. Nature Genet 2006;38:303–311. [PubMed: 16493421]

Pazour GJ, Dickert BL, Vucica Y, Seeley ES, Rosenbaum JL, Witman GB, Cole DG. Chlamydomonas IFT88 and its mouse homologue polycystic kidney disease gene tg737, are required for assembly of cilia and flagella. J Cell Biol 2000;151:709–718. [PubMed: 11062270]

Roberts GJ, Blackwood HJ. Growth of the cartilages of the mid-line cranial base; a radiographic and histological study. J Anat 1983;136:307–320. [PubMed: 6682850]

Rosenbaum JL, Witman GB. Intraflagellar transport. Nature Reviews Mol Cell Biol 2002;3:813–825.

Scherft JP, Daems WT. Single cilia in chondrocytes. J Ultrastruc Res 1967;19:546–555.

Shimazu A, Nah HD, Kirsch T, Koyama E, Leatherman JL, Golden EB, Kosher RA, Pacifici M. Syndecan-3 and the control of chondrocyte proliferation during endochondral ossification. Exp Cell Res 1996;229:126–136. [PubMed: 8940256]

Shimo T, Gentili C, Iwamoto M, Wu C, Koyama E, Pacifici M. Indian hedgehog and syndecan-3 coregulate chondrocyte proliferation and function during chick limb skeletogenesis. Dev Dyn 2004;229:607–617. [PubMed: 14991716]

Singla V, Reiter JF. The primary cilium as the cell's antenna: signaling at a sensory organelle. Science 2006;313:629–633. [PubMed: 16888132]

Sorokin SP. Reconstructions of centriole formation and ciliogenesis in mammalian lungs. J Cell Sci 1968;207:207–230. [PubMed: 5661997]

St-Jacques B, Hammerschmidt M, McMahon AP. Indian hedgehog signaling regulates proliferation and differentiation of chondrocytes and is essential for bone formation. Genes Dev 1999;13:2076–2086.

Stickens D, Zak BM, Rougier N, Esko JD, Werb Z. Mice deficient in Ext2 lack heparan sulfate and develop exostoses. Development 2005;132:5055–5068. [PubMed: 16236767]

Tamamura Y, Otani T, Kanatani N, Koyama E, Kitagaki J, Komori T, Yamada Y, Costantini F, Wasisaka S, Pacifici M, et al. Developmental regulation of Wnt/β-catenin signals is required for growth plate assembly, cartilage integrity, and endochondral ossification. J Biol Chem 2005;280:19185–19195. [PubMed: 15760903]

The I, Bellaiche Y, Perrimon N. Hedgehog movement is regulated through tout-velu-dependent synthesis of a heparan sulfate proteoglycan. Mol Cell 1999;4:633–639. [PubMed: 10549295]

Vortkamp A, Lee K, Lanske B, Segre GV, Kronenberg HM, Tabin CJ. Regulation of rate of cartilage differentiation by Indian hedgehog and PTH-related protein. Science 1996;273:613–622. [PubMed: 8662546]

Xiao Z, Zhang S, Mahlios J, Zhou G, Mangenhelmer BS, Guo D, Dallas SL, Maser R, Calvet JP, Bonewald L, et al. Cilia-like structures and polycystin-1 in osteoblasts/osteocytes and associated abnormalities in skeletogenesis and Runx2 expression. J Biol Chem 2006;281:30884–30895. [PubMed: 16905538]

Yin M, Gentili C, Koyama E, Zasloff M, Pacifici M. Antiangiogenic treatment delays chondrocyte maturation and bone formation during limb skeletogenesis. J Bone Min Res 2002;17:56–65.

Young B, Minugh-Purvis N, Shimo T, St-Jacques B, Iwamoto M, Enomoto-Iwamoto M, Koyama E, Pacifici M. Indian and sonic hedgehog regulate synchondrosis growth plate and cranial base development and function. Dev Biol 2006;299:272–282. [PubMed: 16935278]

Zelzer E, McLean W, Ng YS, Fukai N, Reginato AM, Lovejoy S, D'Amore PA, Olsen BR. Skeletal defects in VEGF(120/120) mice reveal multiple roles of VEGF in skeletogenesis. Development 2002;129:1893–1904. [PubMed: 11934855]

Zhang Q, Murcia NS, Chittenden LR, Richards WG, Michaud EJ, Woychik RP, Yoder BK. Loss of Tg737 protein results in skeletal patterning defects. Dev Dyn 2003;227:78–90. [PubMed: 12701101]

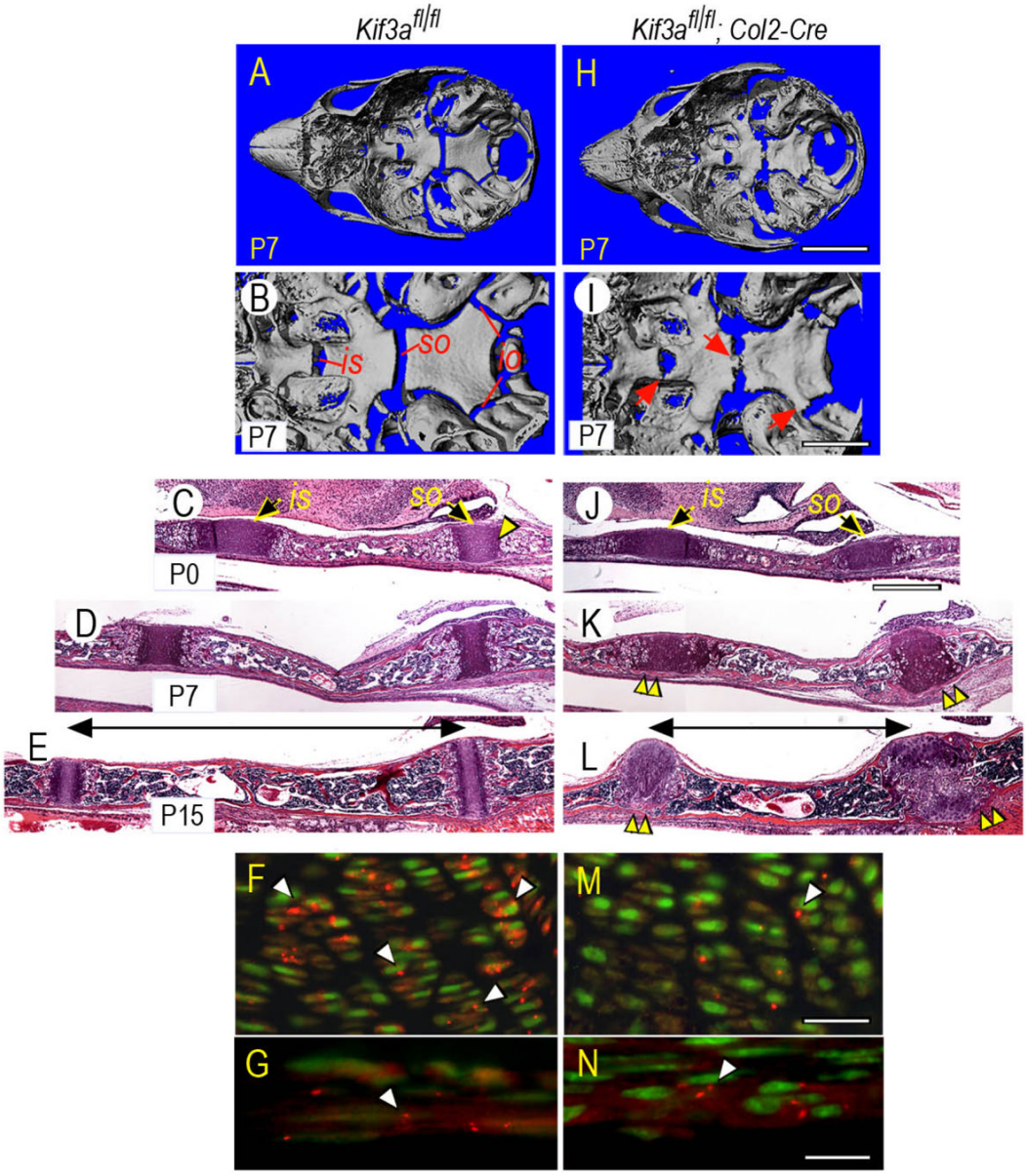

Fig. 1.

Kif-3a-deficient cranial bases and synchondroses are abnormal. (A–B,H–I) Skulls from P7 control (*Kif3a*$^{fl/fl}$) and *Kif3a*-deficient (*Kif3a*$^{fl/fl}$*;Col2-Cre*) mice were analyzed by μCT and are shown by bird-eye view at low and high magnification. Location of intrasphenoidal (*is*), spheno-occipital (*so*) and intra-occipital (*io*) synchondroses is indicated in controls; arrows point to defects in mutant specimens. (C–E,J–L) Parasagittal H&E-stained sections of control and *Kif3a*-deficient cranial bases displaying *is* and *so* synchondroses and intervening endochondral bone. Note that mutant synchondroses' histology and organization are markedly abnormal compared to controls, and distance between the synchondroses is reduced as well (indicated by horizontal line). (F–G,M–N) Immunolocalization of acetylated α-tubulin in primary cilia (arrowheads) in P0 control (F–G) and *Kif3a*-deficient (M–N) synchondrosis growth plate and associated perichondrium. Scale bars: 5 mm for A,H; 2 mm for B,I; 300 μm for C–E and J–L; 100 μm for F,M; and 35 μm for G,N.

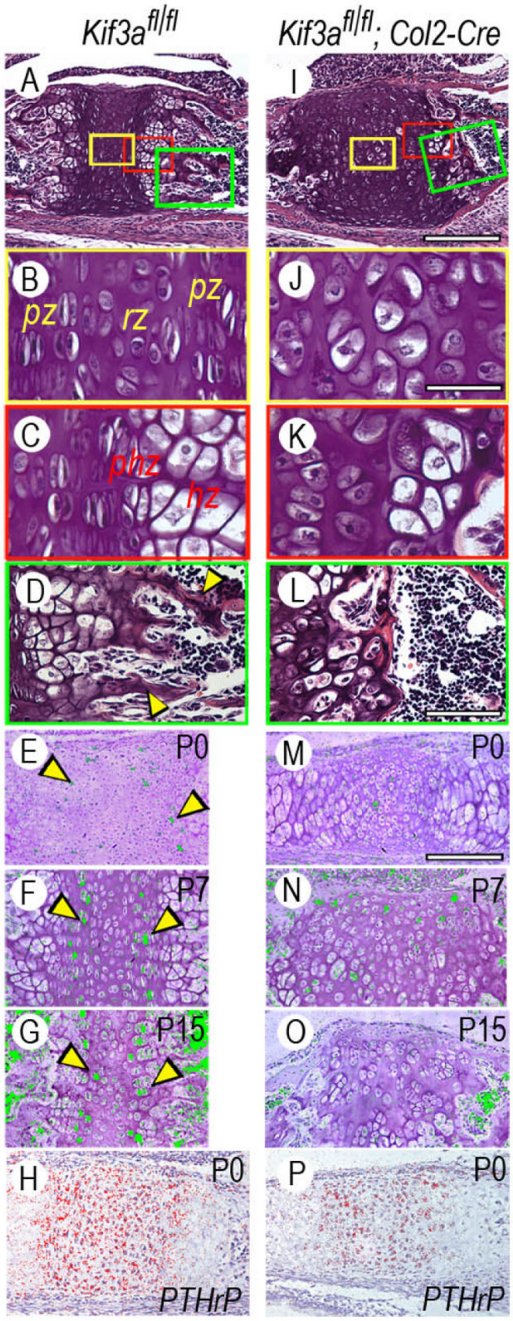

Fig. 2.

Synchondrosis growth plate organization and chondrocyte proliferation are deranged in *Kif3a*-deficient cranial bases. (A–D) Parasagittal sections of P7 control spheno-occipital synchondrosis. Note the presence of resting (*rz*), proliferative (*pr*), pre-hypertrophic (*phz*) and hypertrophic (*hz*) growth plate zones and primary bone spongiosa (arrowheads in D). Boxed colored areas in A are shown at higher magnification in B–D. (E–G) Presence and location of proliferating chondrocytes in control P0, P7 and P15 *so* synchondroses as revealed by *histone 4C* gene expression by in situ hybridization. Hybridization signal was given an artificial color for illustration purpose. Note the presence of two well-defined proliferative zones indicated by arrowheads flanking a central resting zone. (H) *PTHrP* gene expression in control P0

synchondrosis that characterizes resting and proliferative zones. (I–L) Parasagittal sections of P7 *Kif3a*-deficient *so* synchondrosis showing that the growth plate zone structure is totally abnormal (J–K) and that there is a near absence of primary spongiosa (L). (M–O) Near absence of *histone 4C*-expressing proliferating chondrocytes in *Kif3a*-deficient synchondroses. (P) PTHrP gene expression in *Kif3a*-deficient synchondrosis Scale bars: 300 μm for A,I; 40 μm for B,C,J,K; 80 μm for D,L; and 150 μm for E-H and M-P.

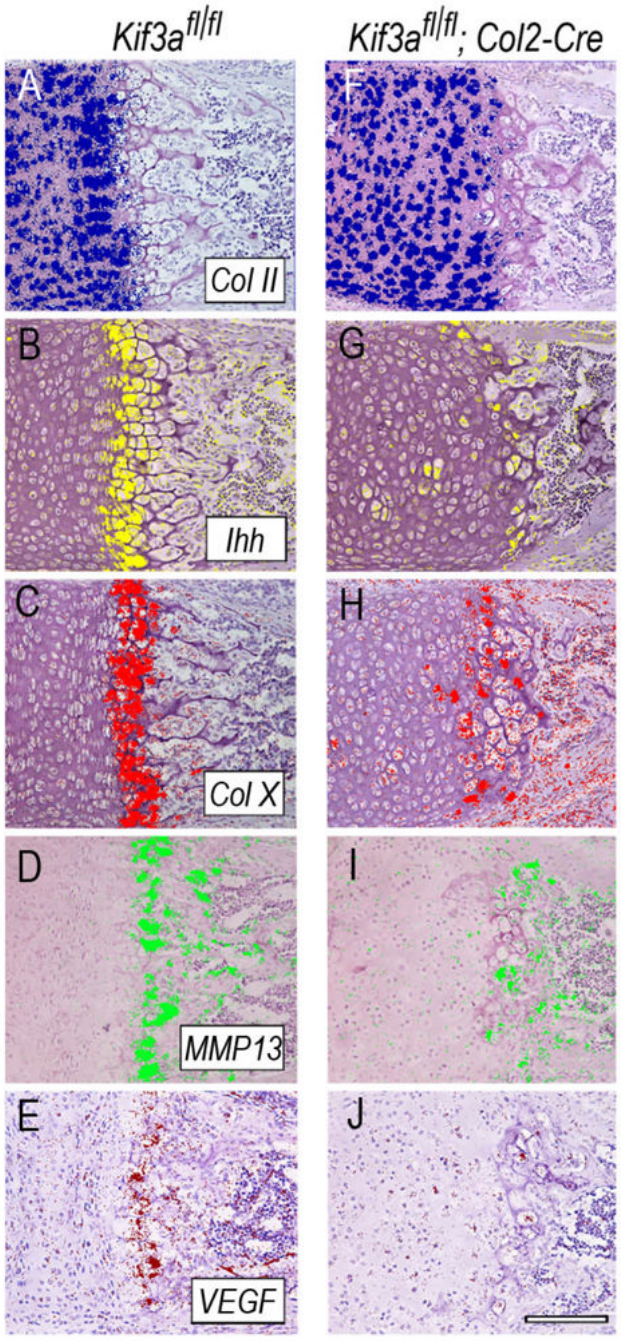

Fig. 3.

Gene expression of chondrocyte maturation-associated genes is depressed in *Kif3a*-deficient synchondroses. Serial sections from the medial portion of P7 control (A–E) and *Kif3a*-deficient (F–J) *so* synchondroses were processed for in situ hybridization analysis of indicated genes, using radiolabeled riboprobes. Hybridization signal was given artificial colors and images were superimposed to hematoxylin histologic images of corresponding field. Scale bar is 100 μm for A–J.

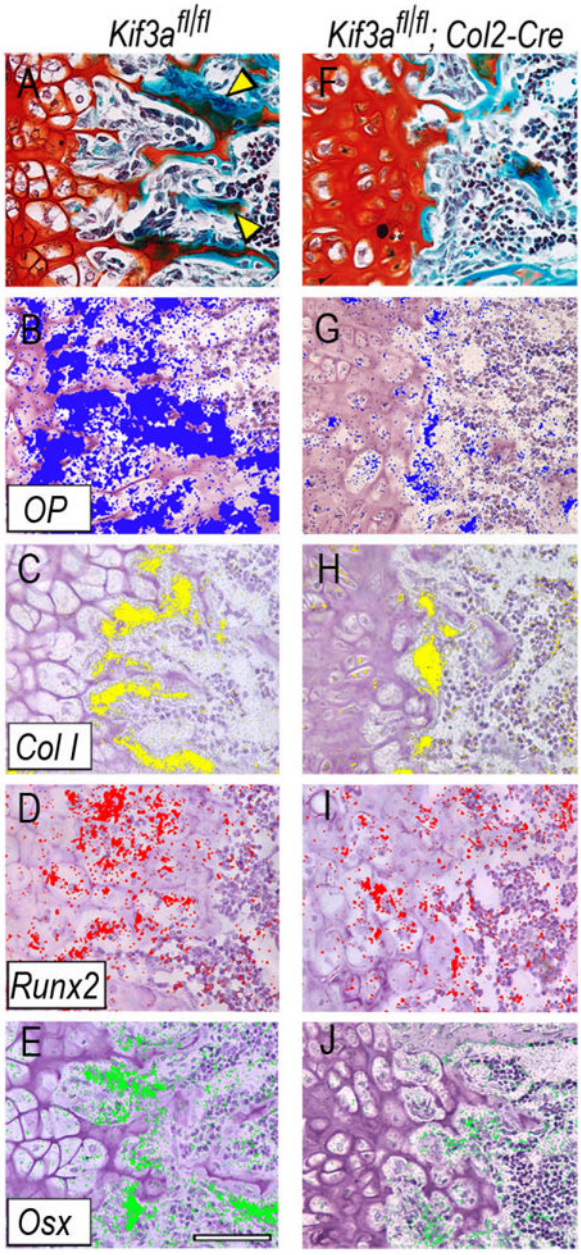

Fig. 4.

Gene expression of cartilage-to-bone-associated genes and formation of primary spongiosa are inhibited in *Kif3a*-deficient synchondroses. (A,F) Parasagittal serial sections of P7 control (A) and mutant *so* synchondrosis (F) were stained with fast green/Safranin O to reveal bone tissue. Note the marked reduction of primary bone spongiosa in mutant tissue (F) that is instead quite clear in controls (A, arrowheads). (B–E) and (G–J) Expression of indicated genes as revealed by in situ hybridization with serial sections of control (B–E) and mutant (G–J) tissue. Scale bar is 80 μm for A–J.

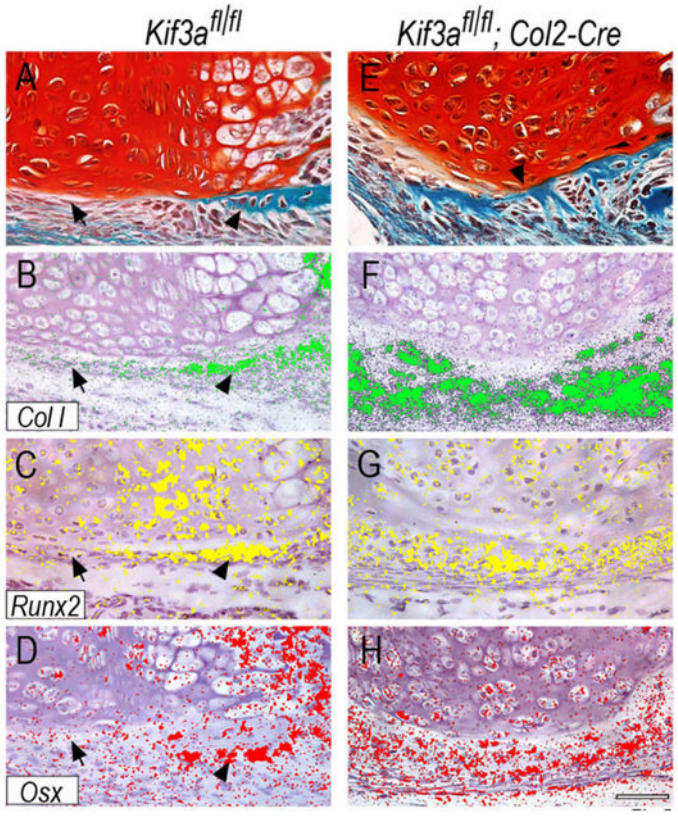

Fig. 5.

Intramembranous ossification is excessive near *Kif3a*-deficient synchondroses. Parasagittal serial sections of P7 control (A–D) and mutant *so* synchondroses were processed for staining with fast green/Safranin O (A,E) or in situ hybridization analysis of indicated genes. Note the presence of intramembranous bone collar adjacent to the pre-hypertrophic and hypertrophic zones in control (A–D, arrowhead) and its absence near the proliferative and resting zones (A–D, arrow) as to be expected. Note instead that intramembranous bone had formed all along the flank of the *Kif3a*-deficient synchondrosis (E–H). Scale bar is 75 μm for A–H.

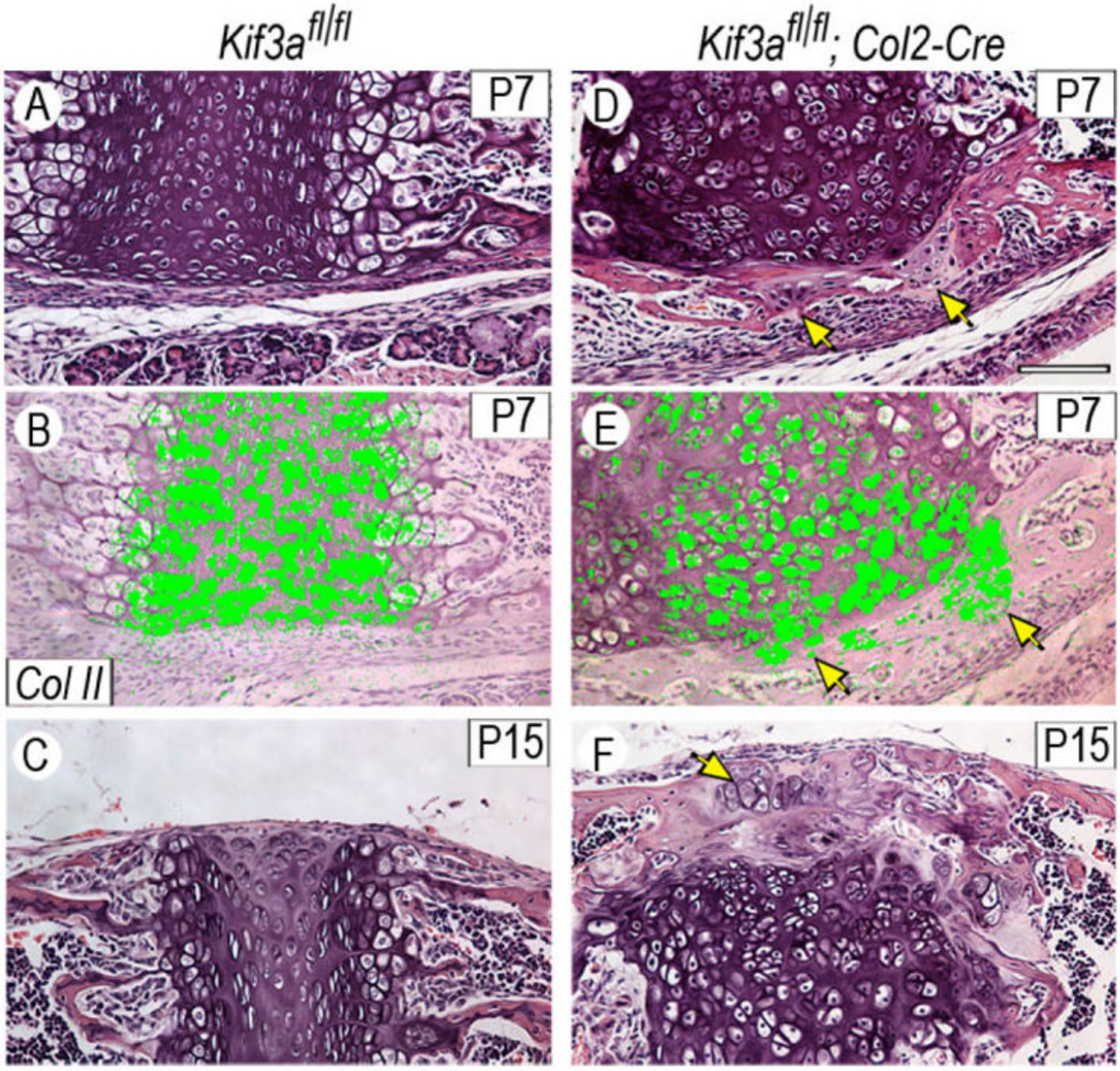

Fig. 6.

Presence of ectopic cartilage masses near *Kif3a*-deficient synchondroses. Sections of P7 and P15 control (A–C) and mutant (D–F) synchondroses were stained with H&E or processed for in situ hybridization analysis of *collagen II* expression. Ectopic cartilaginous masses forming in mutant specimens (arrows in D–E) are recognizable by their typical histology and expression of *collagen II*. Such phenomenon is never observed in control specimens where the chondro-perichondrial boundary is clear and un-violated (A–C). Scale bar is 75 μm for A–F.

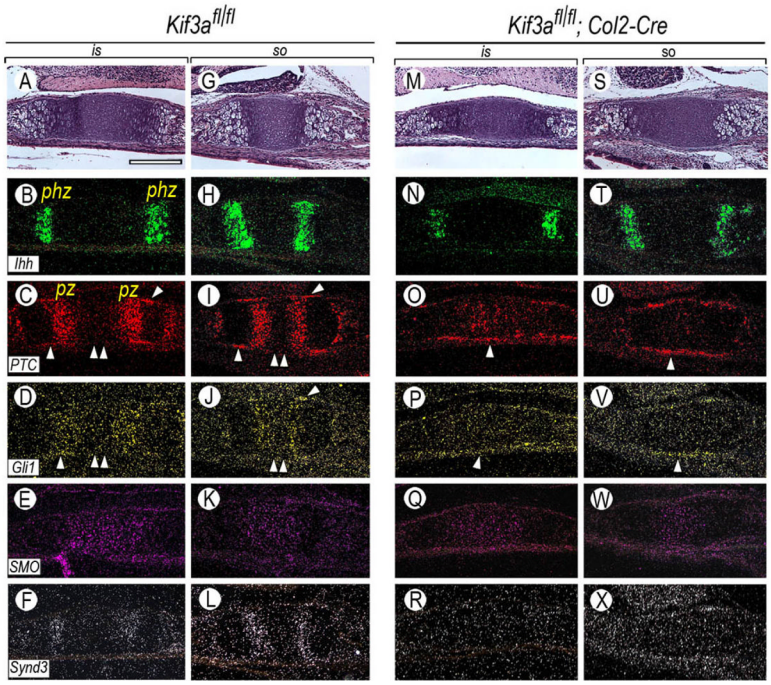

Fig. 7.

Topography of hedgehog signaling is altered in *Kif3a*-deficient synchondroses. Serial section of P0 control (A–L) and mutant (M–X) *is* and *so* synchondroses were processed for expression analysis of indicated genes. Note in controls that *Patched-1* and *Gli-1* are expressed in proliferative zone (*pz*) and perichondrium flanking pre-hypertrophic and hypertrophic zones (C–D, I–J, single arrowhead), but not in perichondrium flanking the resting and proliferative zones (C–D, I–J, double arrowheads). In mutants, however, *Patched-1* and *Gli-1* are minimally expressed within the growth plates, but are expressed all along the perichondrial tissues (O–P, U–V, single arrowhead). Note also that *syndecan-3* expression is mainly restricted to the proliferative zone in controls (F,L), but is extremely low in mutants (R,X). Expression of *Ihh* and *Smoothened* was similar in control (B,H, E,K) and mutant (N,T, Q,W) tissues at this stage. Scale bar is 150 μm for A–X.

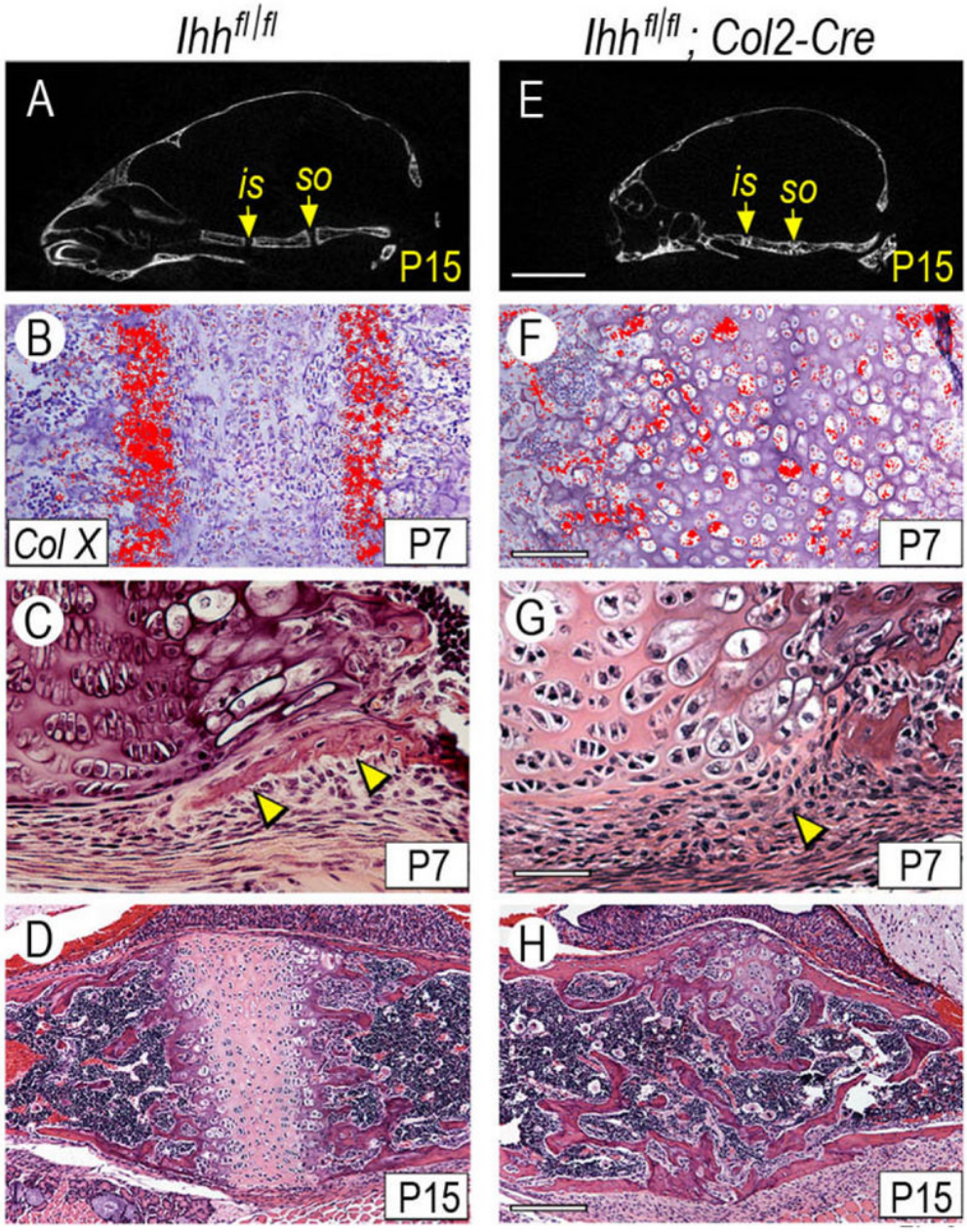

Fig. 8.

Conditional postnatal *Ihh* deficiency causes cranial base abnormalities. (A,E) Skulls from P15 control and *Ihh*-deficient mice were subjected to μCT analysis and one orthogonal plane through the cranial base is shown here. Note the presence of well defined *is* and *so* synchondroses in controls (A, arrows) and the ill-defined synchondroses and reduced antero-posterior length in mutants (E). (B–D, F–H) Sections from P7 and P15 control and mutant *so* synchondroses processed for collagen X gene expression (B,F) or histological analysis (C–D,G–H). Note that collagen X transcripts are restricted to hypertrophic zones in control (B) but are widespread throughout the mutant synchondrosis (F). Note also the presence of a well-formed intramembranous bone collar flanking the pre-hypertrophic and hypertrophic zones in control (C, arrowheads) that is undetectable in mutant (G, arrowhead). Note also that much of

mutant synchondrosis is replaced by endochondral bone by P15 (H). Scale bar is 2 mm for A,E; 150 μm for B,F; 75 μm for C,G; and 250 μm for D,H.